Energy consumption and performance optimisation of laser cleaning for coating removal

Energy consumption and performance optimisation of laser cleaning for coating removal

J. Ouyang[1], P. Mativenga[1*], N. Goffin[3], W. Liu[2], Z. Liu[2], N. Mirhosseini[1], L. Jones[3], E. Woolley[3], L. Li[1]

[1]Department of Mechanical, Aerospace and Civil Engineering, School of Engineering, The University of Manchester, Manchester, M13 9PL, UK
[2]Department of Materials, School of Natural Sciences, The University of Manchester, Manchester, M13 9PL, UK
[3]Wolfson School of Mechanical, Electrical and Manufacturing Engineering, Loughborough University, Leicestershire, LE11 3TU, UK

*Corresponding author: P.Mativenga@manchester.ac.uk

Abstract

Selective removal of coatings by lasers can facilitate the reuse of coated tools in a circular economy. In order to optimise and control the process, it is essential to study the impact of process input variables on process performance. In this paper, coating removal from tooling was carried out using a picosecond a pulsed fibre laser, in order to investigate the effects of laser pulse energy, pulse frequency, galvo scanning speed and scanning track stepover. A fractional factorial design of experiments and analysis of variance was used to optimise the process; considering cleaning rate, specific energy consumption and surface integrity as assessed by changes in surface roughness and composition of the tooling after laser cleaning. The results shows synergy between cleaning rate and specific energy with the laser pulse frequency and galvo scanning speed as the two most significant factors, while the laser pulse energy had the greatest contribution to changes in surface composition. Based on extensive experiments, the relationship between processing rate and system specific energy consumption was mathematically modelled. The paper contributes a new specific energy model for laser cleaning and provides a benchmark of the process energy requirements compared to other manufacturing processes. Additionally, the generic scientific learning from this is that the rate of energy input is a key tool for maximising cleaning rate and minimising specific energy requirements, while the intensity of energy applied, is a key metric that influences surface integrity. More complex factors, influence the surface integrity.

Keywords: laser, selective coating removal, tools, energy consumption, cleaning rate, cobalt binder

1. Introduction

Thin-film coatings have been widely used in the cutting tool industry for improving wear resistance, reducing cutting, reducing heat generation and extending tool life. In a circular economy, reuse of high value tooling can be facilitated by removing the coating, regrinding and re-coating. In many industrial processes, chemical cleaning is used for coating removal [1 -3]. However, concern over the environmental burden of chemical disposal is driving manufacturers to consider chemical-free de-coating approaches.

The use of lasers is a promising approach for selective removal of coatings from tool surfaces. By controlling the laser parameters, it has the potential to minimise substrate damage. Marimuthu et al. [4 - 6], See et al. [7] and Ragusich et al. [8] researched Ti-based coating removal from cemented tungsten carbide substrates by using a nanosecond pulsed KrF excimer laser with 248 nm wavelength, a diode pumped solid state nanosecond pulsed laser at 355 nm wavelength and a femtosecond laser at 800 nm wavelength respectively. While these earlier investigations have evaluated the process capability of coating removal, there is limited understanding of the contribution of key process variables on coating removal rate, and in particular on system energy consumption, which are linked to the energy effectiveness of such processes. Additionally, the carbide tooling has WC as a hard phase held together by a cobalt binder. Detailed understanding of the impact of laser cleaning on cobalt composition is required.

Previous research by Ouyang et al. [9] established the process of removing TiN/TiAlN and TiAlN coating from WC-Co cutting inserts by use of picosecond laser sources. A pulsed fibre laser with 1060 nm wavelength and a diode pumped solid-state laser with 355 nm wavelength were used. The laser de-coating process rate and specific energy consumption were reported.

Within the global manufacturing industry, there is increasing recognition of the need to improve energy efficiency, to reduce both costs and carbon footprint and advance product quality. Also, before applying the coating, the tool surface integrity and chemical condition are the key factors in coating adhesion and wear performance. It is thus timely to understand and optimise the production efficiency, energy consumption and surface quality of the laser de-coating by controlling the processing parameters.

To compare the productivity of different manufacturing processes, Gutowski et al. [10,11] developed a graph of the specific energy consumption in relation to the processing rate. They standardised the assessment by evaluating the specific energy requirements in J/kg and the manufacturing rate in kg/hr for various manufacturing processes. The graph was developed from a review of published literature and this dataset can be used to evaluate how the material processing efficiency of new processes such as laser cleaning compares to the overall family of manufacturing processes.

Kara and Li [12] developed an empirical model to characterise the specific energy consumption in material removal processes. This was tested and validated on a number of turning and milling machine tools. This model concept was further studied by Zhou et al. [13] and Li et al. [14] based on a literature review and a case study. Modelling the specific energy, normalises the analysis and adds a new dimension to understanding the contribution of the production (material process) independent and production dependant energy demand.

In this paper, a pulsed fibre laser with 1060 nm wavelength and 150 ps pulse duration was used to carry out a set of Taguchi experiments on coating removal from cutting inserts. The main process parameters studied were laser pulse energy, pulse frequency, galvo scanning speed and scanning track stepover, in order to investigate the effects on system production efficiency, energy consumption and cobalt content of the carbide after the laser de-coating process. The data generated was used to model the specific energy requirements which was then benchmarked to a published dataset for other manufacturing processes.

2. Experimental Details

2.1. Materials and equipment

Laser de-coating experiments were carried out using an IPG YLPP-1-150V-30 pulsed fibre laser system, with a wavelength of 1060 nm, pulse duration of 150 ps and nominal maximum beam power of 27 W. The laser beam was delivered by using a galvo scanner and focused through an F-theta lens incident onto the workpiece. The laser emits a circular shaped near Gaussian beam output. This was focused to a spot diameter of 50 μm on the focal plane for processing. The cutting tool sample was mounted on a fixed processing stage. The de-coating process was carried out on the laser beam focus plane. Raster scanning of the laser beam was used to overlap between subsequent scanned paths. The cutting tools used were ISCAR CNMA 120408F IC807 WC-Co-based carbide tool inserts coated with TiAlN and TiN/TiAlN. As with previous work by Ouyang et al. [9], the tools were sectioned and assessed to have a ~1.7 μm coating of TiAlN on the tool rake face and ~4.2 μm TiN/TiAlN coating on the flank face.

2.2. Design of experiments

Using the Taguchi experimental design [15] an L9 orthogonal array was selected for the four factors at three levels. The advantage of using an orthogonal array is the ability to estimate all the main factor effects and all the possible interaction from a minimum number of tests. This is considered an efficient experiment since much information is obtained from a few trials

[16]. The analysis of variance (ANOVA) and signal-to-noise ratio of main effects were used to evaluate the relative effect of the input factors on the response metrics and to determine which factor has the highest effect as well as to select a process optimum.

The laser de-coating process was carried out with different laser beam pulse energy of 35 μJ, 40μJ and 45 μJ, pulse frequency 200 kHz, 400 kHz and 600 kHz, galvo scanning speed 3000 mm/s, 6000 mm/s and 9000 mm/s, beam scanned track stepover 5 μm, 10 μm and 15 μm. The track stepover is defined as the offset distance between the previous and next beam path during raster scanning which is controlled by the galvo scanner. The pulse energy levels were chosen in the de-coating processing window to remove the coating without damage to the WC-Co substrate on the insert as established in the previous research by Ouyang et al. [9]. The Taguchi L9 experiment has nine runs and each run was repeated three times to establish repeatability giving 27 runs in total. The runs were run at random. In each run, the galvo repeat scan times vary to maintain the same total laser number of pulses (NOP) at 80000 pulses per mm^2 delivered to the workpiece under each test condition. The laser system was used to create de-coating tracks on both flank and rake faces. At the rake face, the TiAlN coating was fully removed, this surface was assessed for the surface roughness and element composition. At the flank face, the TiN/TiAlN coating was partially removed, the coating volume removed was measured to calculate the de-coating processing rate.

2.3. Measurements and Response Evaluation

In this study, de-coating processing rate, specific energy consumption of the full laser system, de-coated surface roughness ***Ra***, and elemental composition in Ti, O, Co of the cleaned surface were investigated. The following section describes in detail the associated measurements and calculations.

De-coating processing rate: This is the coating removal rate in cm^3/s during laser processing and therefore represents the system's de-coating productivity. The optimisation goal is to increase the processing rate and hence reduce cycle time which should also reduce energy consumption. The processing rate $\boldsymbol{Q}$ was calculated by equation 1:

$$\boldsymbol{Q} = \frac{\boldsymbol{V}}{\boldsymbol{t}} \tag{1}$$

Where $\boldsymbol{V}$ is the volume of coating removed and $\boldsymbol{t}$ is the processing time with units of cm^3 and s respectively. The volume of coating removed was measured by a Veeco ContourGT white light interferometer. The processing time was logged for each test run.

System specific energy consumption (SEC): This is the energy consumed normalised by the volume of coating removed, with units of MJ/cm^3. In this research, energy consumption was only electrical, without any other type of energy input. The goal is to decrease the system specific energy consumption and improve energy effectiveness. The specific energy consumption $\boldsymbol{E_{SEC}}$ was calculated by equation 2:

$$\boldsymbol{E_{SEC}} = \frac{\boldsymbol{P}}{\boldsymbol{Q}} \tag{2}$$

Where $\boldsymbol{P}$ is the system active power drawn in the processing stage, which is the actual electrical power load on the system, and was measured by a Fluke 434 power analyser for each test run. The processing rate is as defined before.

Surface roughness: The arithmetic mean surface roughness $\boldsymbol{Ra}$, in μm was measured by the Veeco ContourGT white light interferometer. For each run, 3 measurements were carried out in different positions, the average value was taken for the final response.

Surface elements composition: The rake face de-coated areas were also analysed by a Zeiss Ultra 55 scanning electron microscope (SEM). The elemental compositional changes by atomic % after laser de-coating were evaluated by energy dispersive X-ray (EDX) analysis which is integrated in the SEM. The tool was also sectioned, and the composition of the uncoated carbide was used to provide a reference.

Substrate residual stress: The substrate residual stress was analysed on the rake face de-coated areas by an X-ray diffraction instrument (Proto iXRD Combo).

In this research, all the response data were analysed by Minitab software using Taguchi designs and Analysis of variance (ANOVA).

3. Results analysis and Discussions

The results for all the responses are summarised in Table 1 together with the L9 experiment parameters. Each output response is discussed in the following section. Figure 1 shows an example of the surface assessment for the trial No. 6b.

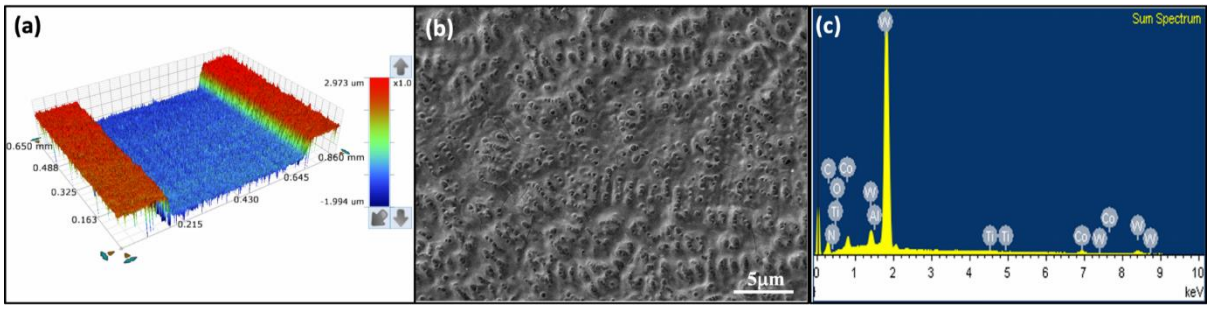

Figure 1 surface assessment of trial No. 6b: (a) 3D surface profile; (b) SEM image; (c) EDX spectrum.

Table 1 Laser de-coating parameters and output responses

Trials No.	Pulse energy (μJ)	Pulse frequency (kHz)	Scanning speed (mm/s)	Stepover (μm)	Processing rate (cm^3/s)	System SEC (MJ/cm^3)	Rake face surface roughness ***Ra*** (μm)	O atomic %	Ti atomic %	Co atomic %
1a	35	200	3000	5	3.25E-06	100.79	0.169	2.93%	1.10%	11.05%
1b	35	200	3000	5	3.30E-06	99.20	0.180	4.28%	1.49%	11.32%
1c	35	200	3000	5	3.55E-06	92.15	0.199	4.14%	2.24%	11.25%
2a	35	400	6000	10	4.99E-06	71.81	0.171	1.68%	1.12%	10.88%
2b	35	400	6000	10	4.67E-06	76.83	0.182	3.12%	1.25%	11.92%
2c	35	400	6000	10	4.76E-06	75.41	0.189	3.23%	1.63%	11.45%
3a	35	600	9000	15	5.65E-06	69.06	0.203	2.21%	1.16%	11.17%
3b	35	600	9000	15	5.32E-06	73.37	0.199	5.68%	1.28%	10.30%
3c	35	600	9000	15	5.41E-06	72.05	0.204	2.44%	2.46%	11.37%
4a	40	200	6000	15	2.67E-06	124.41	0.204	2.03%	0.60%	11.59%
4b	40	200	6000	15	2.43E-06	136.52	0.205	2.03%	0.60%	11.59%
4c	40	200	6000	15	2.40E-06	138.40	0.217	3.27%	1.28%	12.23%
5a	40	400	9000	5	3.94E-06	93.36	0.186	3.11%	0.65%	11.41%
5b	40	400	9000	5	3.95E-06	92.98	0.197	4.01%	0.88%	11.62%
5c	40	400	9000	5	3.65E-06	100.68	0.195	3.35%	0.98%	11.98%
6a	40	600	3000	10	1.14E-05	35.33	0.166	2.50%	0.21%	11.29%
6b	40	600	3000	10	1.08E-05	37.29	0.181	3.58%	0.45%	11.26%
6c	40	600	3000	10	1.03E-05	39.14	0.178	3.45%	0.64%	11.21%
7a	45	200	9000	10	2.16E-06	155.83	0.208	3.01%	0.27%	11.63%
7b	45	200	9000	10	2.11E-06	159.07	0.216	4.56%	0.58%	11.96%
7c	45	200	9000	10	2.07E-06	162.73	0.214	3.17%	0.73%	12.82%
8a	45	400	3000	15	8.29E-06	45.45	0.194	2.19%	0.08%	11.97%
8b	45	400	3000	15	7.85E-06	48.01	0.208	2.19%	0.08%	11.97%
8c	45	400	3000	15	7.65E-06	49.26	0.207	3.05%	0.44%	11.74%
9a	45	600	6000	5	8.63E-06	48.31	0.170	3.68%	0.37%	10.29%
9b	45	600	6000	5	7.81E-06	53.42	0.190	3.70%	0.51%	11.19%
9c	45	600	6000	5	7.63E-06	54.69	0.215	4.56%	0.45%	10.74%

Note: a, b, c represent repeats of experimental runs

3.1. Analysis of processing rate

Figure 2 shows the response graph for signal-to-noise ratio (S/N) of the de-coating processing rate. The objective is to maximise the processing rate. Each value along the x-axis corresponds to the three levels for a particular factor. The gradient of the line indicates the degree to which a particular factor has a dominant effect on the performance output. Based on the gradient from Figure 2, it is clear that the most dominant contributing input factor for processing rate is made by the pulse frequency, followed by the scanning speed.

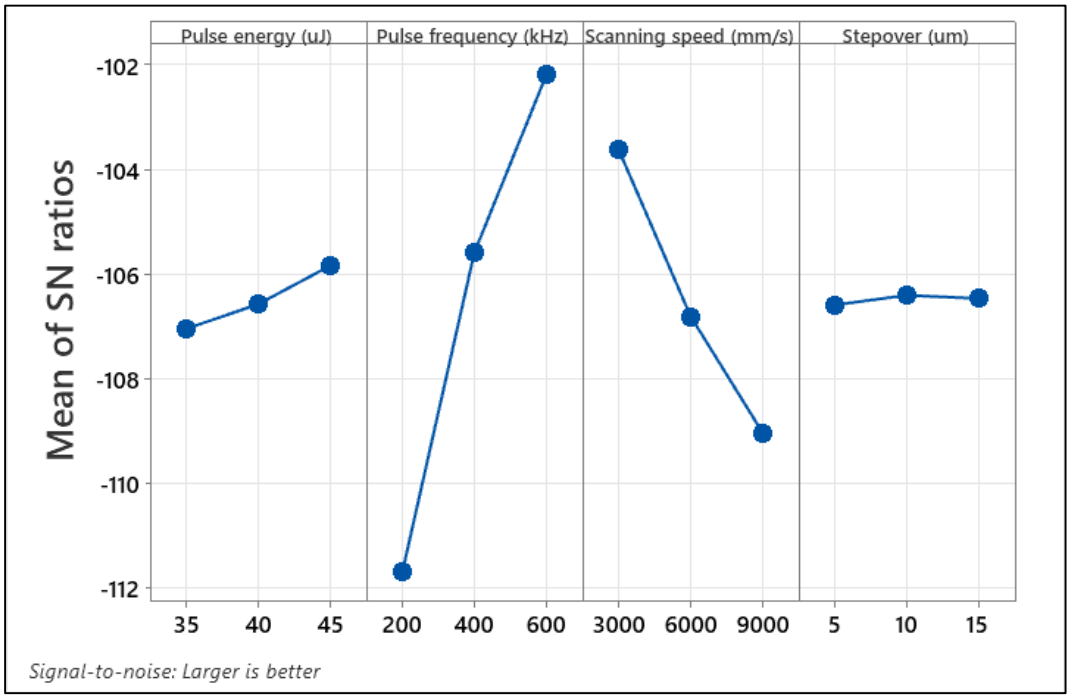

Figure 2 Factors that dominate processing rate as assessed by signal-to-noise ratio main effects plots (S/N)

To quantify the contribution of factors to the processing rate, the analysis of variance (ANOVA) was performed. The ANOVA result for the processing rate is shown in Table 2. The contribution percentage indicates the relative ability of a factor to affect the response.

Table 2 Analysis of variance processing rate

Source	DF	Seq SS	Contribution	Adj SS	Adj MS	F-Value	P-Value
Pulse energy (uJ)	2	0.089	1.19%	0.089	0.044	21.07	0.000
Pulse frequency (kHz)	2	5.546	74.45%	5.546	2.773	1315.60	0.000
Scanning speed (mm/s)	2	1.774	23.82%	1.774	0.887	420.88	0.000
Stepover (um)	2	0.002	0.03%	0.002	0.001	0.45	0.645
Error	18	0.038	0.51%	0.038	0.002		
Total	26	7.449	100.00%				

Based on Figure 2 and Table 2, the most effective variable to control the processing rate is the pulse frequency with 74.45% contribution and the steepest gradient. The scanning speed is

the second, ranked with 23.82% contribution. The Error in Table 2 is 0.51% contribution, which indicates that no important factors are omitted from the experiments. The "p-value" is a probability that the evidence against the null hypothesis, normally if the "p-value" is less than the significance level of 0.05, it indicates that there is a statistically significant association between the response characteristic and the term. In this case the "p-value" of stepover is 0.645 which indicates this factor is not significant with respect to the processing rate response. The optimal factor-level combination was using the highest pulse energy of 45 μJ, the highest pulse frequency of 600 kHz, and the lowest scanning speed of 3000 mm/s for the galvo and 10 μm for stepover. This is identified by picking the highest points in Figure 2, i.e. maximising the signal-to-noise ratio.

The scientific rationale for this finding is that the higher the pulse frequency, the more laser pulses are incident on the sample in one second, and the higher the energy input rate, which intensifies the laser-material interaction during processing, hence increasing the processing rate [17-18]. The preferable lower scanning speed means more beam overlap and higher energy delivery which leads to more heat accumulation in a localised area, hence enhances the incubation effect [19], but with a lower contribution compared to the pulse frequency impact.

3.2. Analysis of system specific energy consumption

The signal-to-noise ratio for system specific energy consumption for a "smaller is better" objective is shown in Figure 3, and the ANOVA analysis is shown in Table 3.

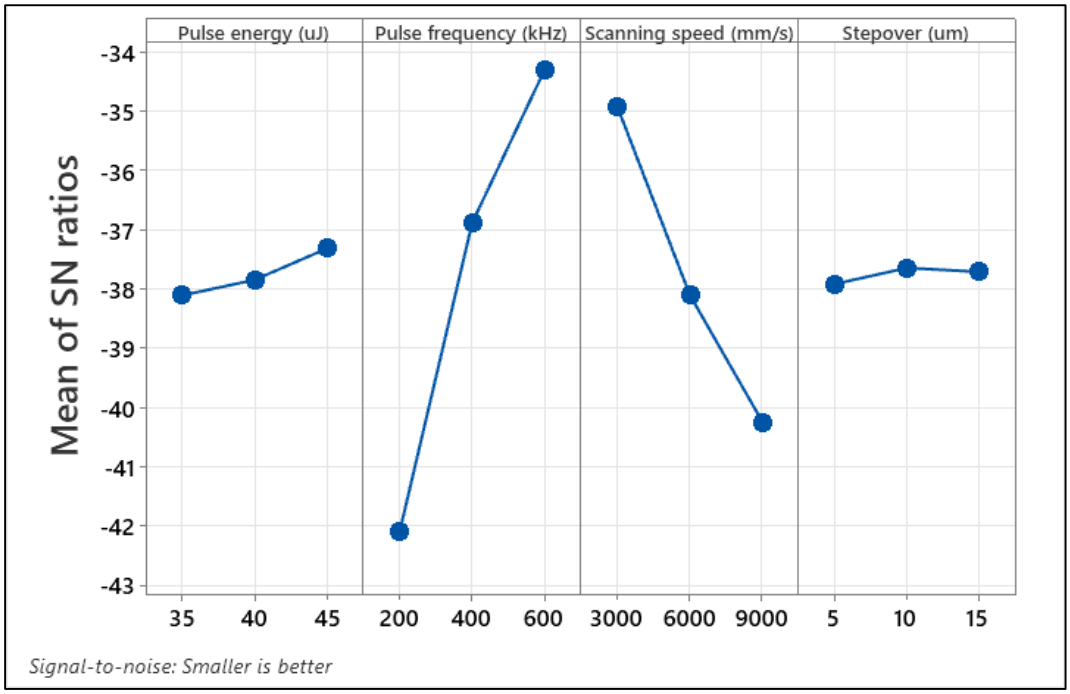

Figure 3 Signal-to-noise ratio of main effects plots for system specific energy consumption

Table 3 Analysis of variance for system specific energy

Source	DF	Seq SS	Contribution	Adj SS	Adj MS	F-Value	P-Value
Pulse energy (uJ)	2	0.039	0.71%	0.039	0.020	9.34	0.002
Pulse frequency (kHz)	2	3.780	67.73%	3.780	1.890	896.69	0.000
Scanning speed (mm/s)	2	1.720	30.81%	1.720	0.860	407.91	0.000
Stepover (um)	2	0.005	0.08%	0.005	0.002	1.07	0.364
Error	18	0.038	0.68%	0.038	0.002		
Total	26	5.582	100.00%				

Similar to the processing rate, the strongest factor of system specific energy consumption was the pulse frequency, but with a 67.73% contribution. Scanning speed was second ranked with 30.81% contribution. The optimal factor-level combination was 45 μJ for pulse energy, 600 kHz for pulse frequency, 3000 mm/s for galvo scanning speed, and 10 μm for stepover. This optimal condition is the same with the processing rate analysis. As the system specific energy consumption is strongly influenced by the processing rate, the higher processing rate leads to higher material removal per unit time, resulting in lower cycle time and reduced energy consumption.

3.3. Analysis of de-coated surface roughness

The mean of rake surface roughness ***Ra*** and ANOVA analysis is shown in Figure 4 and Table 4 respectively.

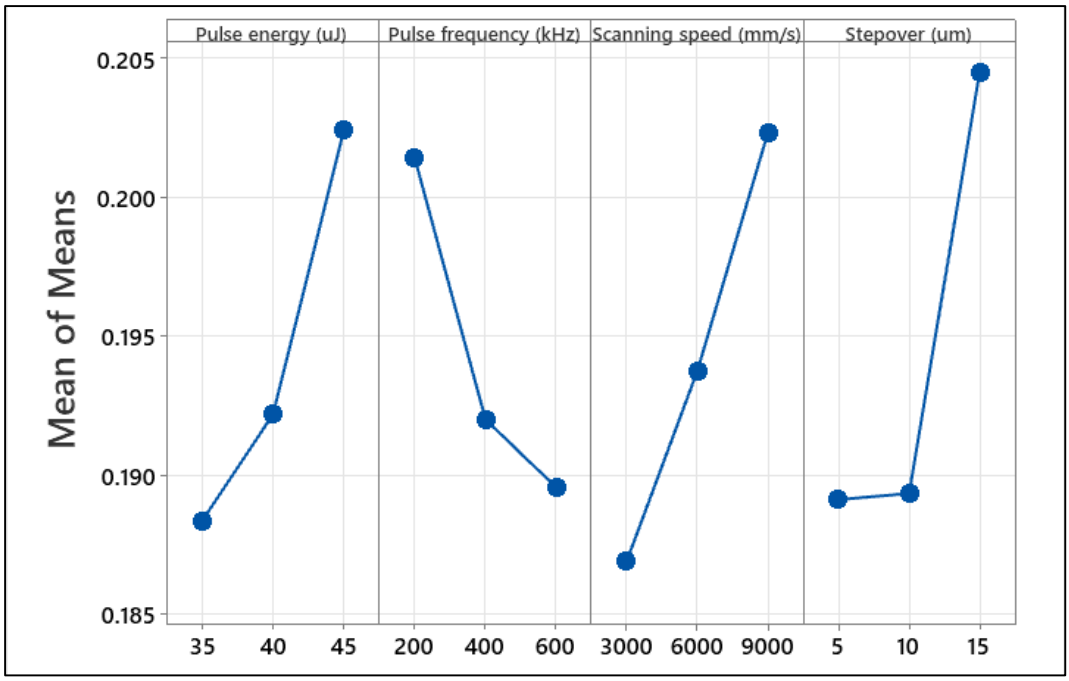

Figure 4 Mean of main effects plot for de-coated surface roughness ***Ra***

Table 4 Analysis of variance for de-coated surface roughness ***Ra***

Source	DF	Seq SS	Contribution	Adj SS	Adj MS	F-Value	P-Value
Pulse energy (uJ)	2	0.001	16.68%	0.001	0.001	4.51	0.026
Pulse frequency (kHz)	2	0.001	12.49%	0.001	0.000	3.38	0.057
Scanning speed (mm/s)	2	0.001	16.35%	0.001	0.001	4.42	0.027
Stepover (um)	2	0.001	21.22%	0.001	0.001	5.74	0.012
Error	18	0.002	33.26%	0.002	0.000		
Total	26	0.006	100.00%				

It was found that the strongest factor governing surface roughness in the four parameters was the beam stepover with 21.22% contribution. Pulse energy and scanning speed had a contribution of 16.68% and 16.35% respectively, while pulse frequency had a 12.49% contribution. However, the error in Table 4 is 33.26%; even higher than the stepover's contribution, which indicates that some other factors would need to be considered to fully understand the changes.

Higher stepover, higher scanning speed and lower pulse frequency would reduce the pulse overlap. Due to geometric footprint of the laser beam, the Gaussian beam profile influences the topography of the surface and ablated profile and, hence increases the surface roughness. This phenomenon is consistent with the research by Liu et al. [20]. Higher pulse energy leads to deeper ablation depth in the centre of incident laser beam, which intensifies the effect of Gaussian beam, and hence increase the surface roughness.

For comparison, the original coated surface roughness ***Ra*** was measured as 0.168±0.039 μm. The range of ***Ra*** after de-coating an area as shown in Table 1 was 0.166 to 0.215. The user can select to maximise or minimise the surface roughness by using the relative processing parameters in the above analyses for particular objective purposes. A smoother surface may be desirable for tooling that is going to be re-used without re-coating, while a rougher surface may help in coating adhesion.

3.4. Analysis of de-coated surface chemical elements composition

The residual Ti element level indicates the cleanness of the surface after laser cleaning, the less Ti atomic % represents the higher surface cleanness. The main effects plot for the Ti atomic % remaining after cleaning with "smaller is better" objective and ANOVA analysis is shown in Figure 5 and Table 5 respectively.

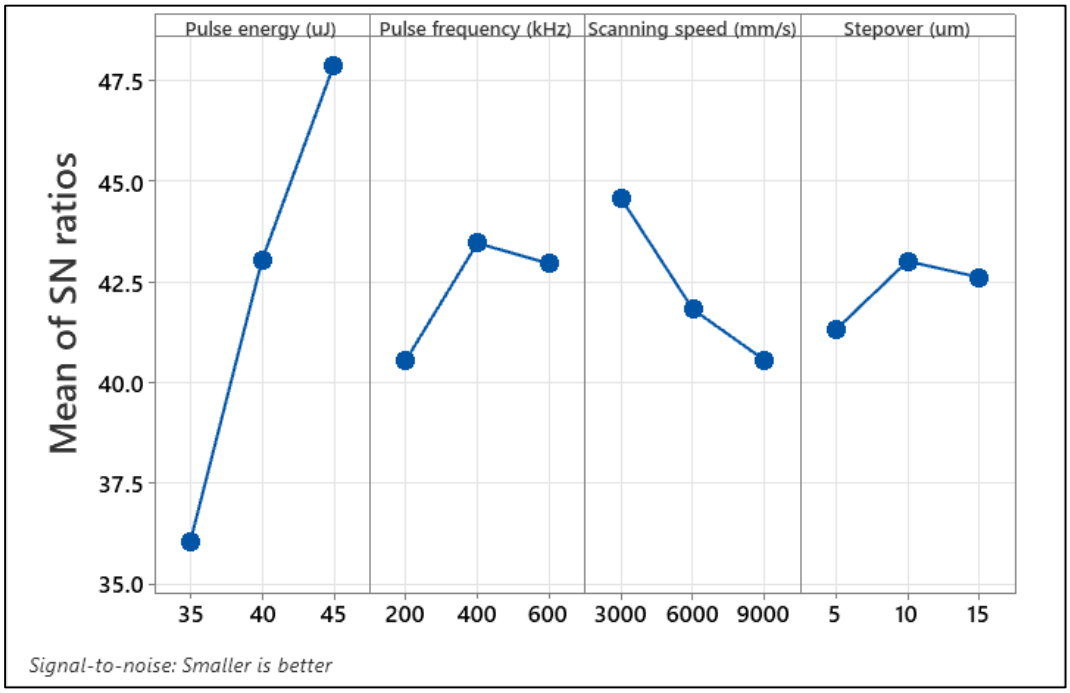

Figure 5 Main effects plot for Ti atomic % S/N ratios

Table 5 Analysis of variance for response of Ti atomic %

Source	DF	Seq SS	Contribution	Adj SS	Adj MS	F-Value	P-Value
Pulse energy (uJ)	2	0.018	66.76%	0.018	0.009	27.53	0.000
Pulse frequency (kHz)	2	0.001	2.95%	0.001	0.000	1.22	0.320
Scanning speed (mm/s)	2	0.002	6.26%	0.002	0.001	2.58	0.103
Stepover (um)	2	0.001	2.19%	0.001	0.000	0.90	0.423
Error	18	0.006	21.83%	0.006	0.000		
Total	26	0.027	100.00%				

It was found that the strongest factor to influence the residual Ti atomic percentage was the pulse energy with 66.76% contribution, while contribution of pulse frequency, scanning speed and stepover were all less than 7%. The optimal factor-level combination was 45 μJ for pulse energy, 400 kHz for pulse frequency, 3000 mm/s for galvo scanning speed, 10 μm for stepover. The error in Table 5 indicates that some other factors need to be considered to better control the surface composition. The scientific rationale for this is that higher pulse energy laser beam in the incident laser beam will lead to rapid temperature rise, promoting coating removal. Hence less Ti residue is detected on the surface.

The lower O atomic percent (%) after laser cleaning represents reduced thermal effects during processing, which is ideal and leads to minimum surface mechanical property change. The main effects plot for O atomic % S/N ratios with “smaller is better” option and ANOVA analysis is shown in Figure 6 and Table 6 respectively.

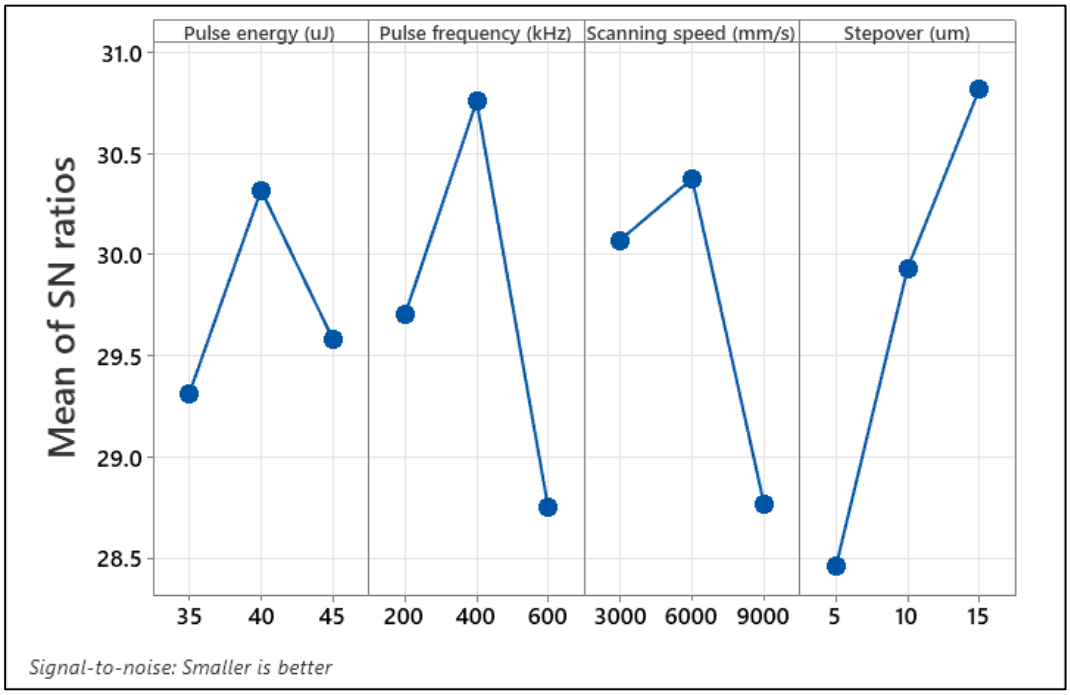

Figure 6 Main effects plot for O atomic % S/N ratios

Table 6 Analysis of variance for response of O atomic %

Source	DF	Seq SS	Contribution	Adj SS	Adj MS	F-Value	P-Value
Pulse energy (uJ)	2	0.037	1.67%	0.037	0.019	0.24	0.786
Pulse frequency (kHz)	2	0.171	7.70%	0.171	0.086	1.13	0.345
Scanning speed (mm/s)	2	0.107	4.79%	0.107	0.053	0.70	0.509
Stepover (um)	2	0.542	24.37%	0.542	0.271	3.57	0.049
Error	18	1.366	61.46%	1.366	0.076		
Total	26	2.223	100.00%				

It was found that the strongest factor of O atomic % was the stepover with 24.37% contribution, while the contribution of pulse energy, pulse frequency and scanning speed are all less than 8%. The error in Table 6, indicates that similar to the Ti composition the control of oxygen content is influenced by other factors beyond the measured laser processing factors. The higher stepover decreases pulse overlap in each scanning track, leading to less heat accumulation in the processing area and lower oxidisation. For comparison, some original inserts without laser de-coated were sectioned mechanically and the cross-sectional area were assessed by the EDX, the O atomic % in the cross section was 5.11%±0.61%. The range of O atomic % in the de-coated area in Table 1 is 1.68% - 5.68%, which is no significant increase of the O atomic % after laser de-coating. In most test conditions after laser de-coating, the O level is actually decreased, which indicates the mechanism of laser de-coating by this laser is mainly vaporisation with less thermal effect.

The main effects plot for Co atomic % S/N ratios with "smaller is better" objective and ANOVA analysis is shown in Figure 7 and Table 7 respectively.

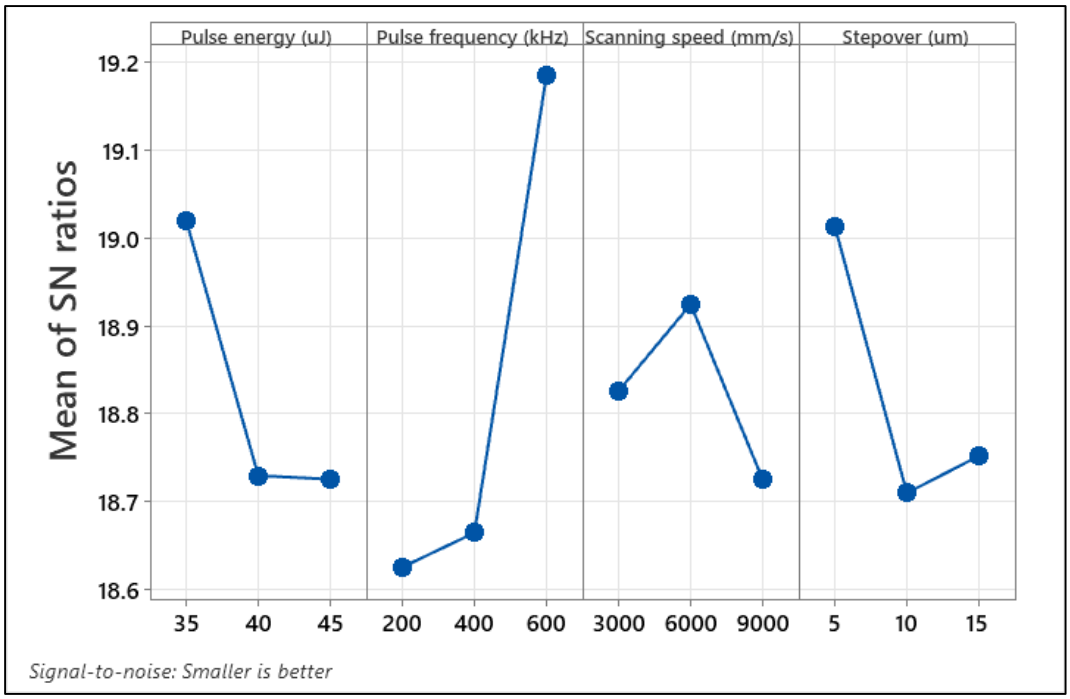

Figure 7 Main effects plot for Co atomic % S/N ratios

Table 7 Analysis of variance for response of Co atomic %

Source	DF	Seq SS	Contribution	Adj SS	Adj MS	F-Value	P-Value
Pulse energy (uJ)	2	0.000	11.70%	0.000	0.000	2.93	0.079
Pulse frequency (kHz)	2	0.000	38.01%	0.000	0.000	9.53	0.002
Scanning speed (mm/s)	2	0.000	3.93%	0.000	0.000	0.98	0.393
Stepover (um)	2	0.000	10.44%	0.000	0.000	2.62	0.101
Error	18	0.000	35.92%	0.000	0.000		
Total	26	0.001	100.00%				

It was found that the strongest factor of Co atomic % was the pulse frequency, with 38.01% contribution. Pulse energy and stepover had nearly the same contribution 11.70% and 10.44% in second and third rank respectively. The optimal factor-level combination was 35 μJ for pulse energy, 600 kHz for pulse frequency, 6000 mm/s for galvo scanning speed, 5 μm for stepover. The Error in Table 7 is 35.92%, indicating that some other factors influence the cobalt content. For comparison, the Co atomic % in the cross section of original inserts is 17.15%±0.80%. The range of Co atomic % after de-coated in Table 1 is 10.73% - 11.97%, which indicates significant decrease of the Co level after laser de-coating. The decrease in cobalt content is an objective pursued by other researchers such as Balleta et al. [21], in order to improve the bonding of chemical vapour deposition (CVD) diamond coating.

3.5 Analysis of surface residual stress after de-coating

The WC-Co substrate rake face residual stresses were measured by the X-ray diffraction instrument (Proto iXRD Combo). The residual stress were evaluated for the Taguchi array. The residual stress was compared to that of the coated and uncoated substrates. The measured results are shown in Figure 8.

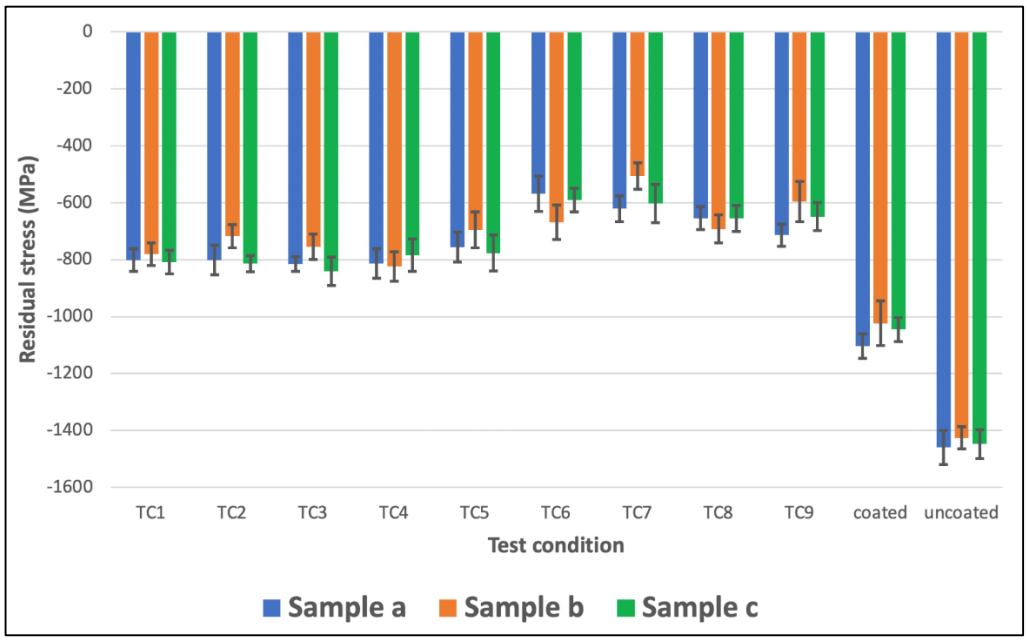

Figure 8 WC-Co substrate rake surface residual stress in each test condition.

From Figure 8, the uncoated carbide tool had significant compressive residual stress from the tool manufacturing process chains. There was about 300 MPa stress relief after PVD coating process. With further laser de-coating process, the surface the magnitude of the compressive was further reduced over all test conditions. This is consistent with other research results on laser coating removal process [22,23], where it was reported that laser ablation of ceramic coating resulted in thermal load on the coating and substrate, tensile stress was created by coating de-bonding.

Residual stresses influence the performance of the cutting tools and may determine the tool life decisively. The compressive residual stress in the substrate surface can avoid cohesive tool damage and slow down crack growth on the tool when machining. In contrast, tensile residual stress enables crack formation and propagation [24, 25]

The objective after laser de-coating should be to minimize the reduction in compressive tensile strength. With this objective, the coated substrate surface residual stress was set as a

reference, the residual stress relief changes in different test condition were assessed by the Taguchi and ANOVA analysis. The results are shown in Figure 9 and Table 8.

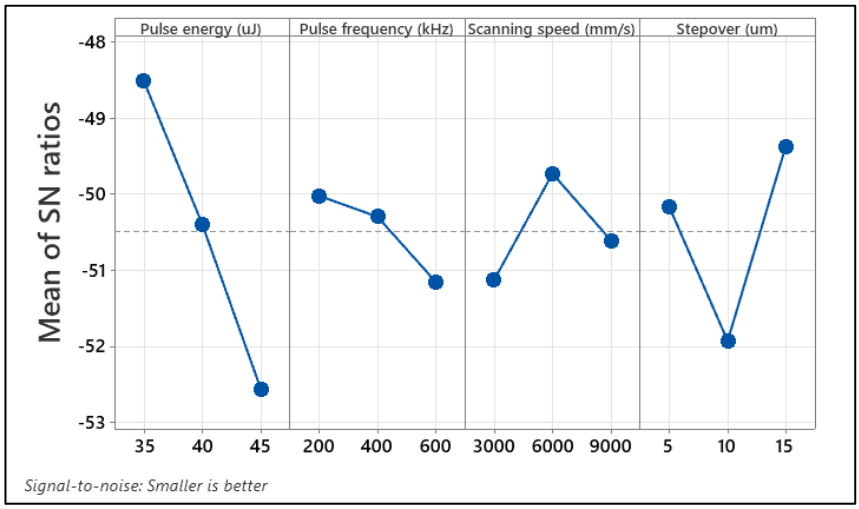

Figure 9 Main effects plot for residual stress changes

Table 8 Analysis of variance for response of residual stress changes relative to coated tool

Source	DF	Seq SS	Contribution	Adj SS	Adj MS	F-Value	P-Value
Pulse energy (uJ)	2	85.410	50.05%	85.410	42.705	23.71	0.000
Pulse frequency (kHz)	2	6.575	3.85%	6.575	3.287	1.83	0.190
Scanning speed (mm/s)	2	9.882	5.79%	9.882	4.941	2.74	0.091
Stepover (um)	2	36.357	21.31%	36.357	18.178	10.09	0.001
Error	18	32.417	19.00%	32.417	1.801		
Total	26	170.641	100.00%				

It was found that the strongest factor governing surface residual stress among the four parameters was the pulse energy with 50.05% contribution. Step over was the second highest contribution at 21.31%. The optimal factor-level combination was 35 μJ for pulse energy, 200 kHz for pulse frequency, 6000 mm/s for galvo scanning speed, 15 μm for stepover. The lower pulse energy and pulse frequency provides less thermal load on the substrate and hence less residual stress relief. However, the optimal factors level for residual stress are not the same as the ones for maximizing the de-coating rate and minimizing the energy consumption. However given that all the de-coated samples had compressive residual stress, a sub-optimum solution for compressive residual stress, selected by maximizing cleaning rate and minimizing energy consumption still provides a strong compressive stress for tooling performance.

3.6 Analysis of optimal factors

In the above section 3.1-3.5, all the single response in the Taguchi array was analysed. In summary all the factors with its optimal values are in Table 9.

Table 9 summary of factors optimal value

	Optimisation Goal	Pulse energy (μJ)	Pulse frequency (kHz)	scanning speed (mm/s)	stepover (μm)
Processing rate	**Larger** is better	45	600	3000	10
System SEC	**Smaller** is better	45	600	3000	10
Ti atomic %	**Smaller** is better	45	400	3000	10
O atomic %	**Smaller** is better	40	400	6000	15
Co atomic %	**Smaller** is better	35	600	6000	5
Residual stress change	**Smaller** is better	35	200	6000	15

In Table 2-8, the response variances of processing rate, system specific energy consumption had higher confidence of control from the input parameters and while the composition and surface roughness had lower confidence as shown in the ANOVA analysis. A theory to consider is that processing temperature and bond energies could be among key variables for the selective removal of the elements.

Optimized parameters intended for reducing energy consumption while maximising cleaning rate were selected to undertake another three runs of laser de-coating. The parameters used were 45 μJ for pulse energy, 600 kHz for pulse frequency, 3000 mm/s for galvo scanning speed, 10 μm for stepover. After measurement and calculation, the processing rate was 1.18±0.05E-05 cm^3/s, system specific energy consumption was 35.24± 1.39 MJ/cm^3, which was 9% increase and 5.5% decrease respectively comparing with the best performance result in Table 1 trial No. 6. The surface roughness was 0.185±0.017 μm, while Ti, O and Co atomic % were 0.23%±0.11%, 3.77%±0.50% and 10.39%±0.71% respectively.

For further investigating the surface integrity changes after laser de-coating, the optimised parameters were selected to de-coat the rake face. The surface chemical elements composition and residual stress were measured after laser repeated scans, the results are shown in Figure 10 and Figure 11. Each test condition was repeated 3 runs.

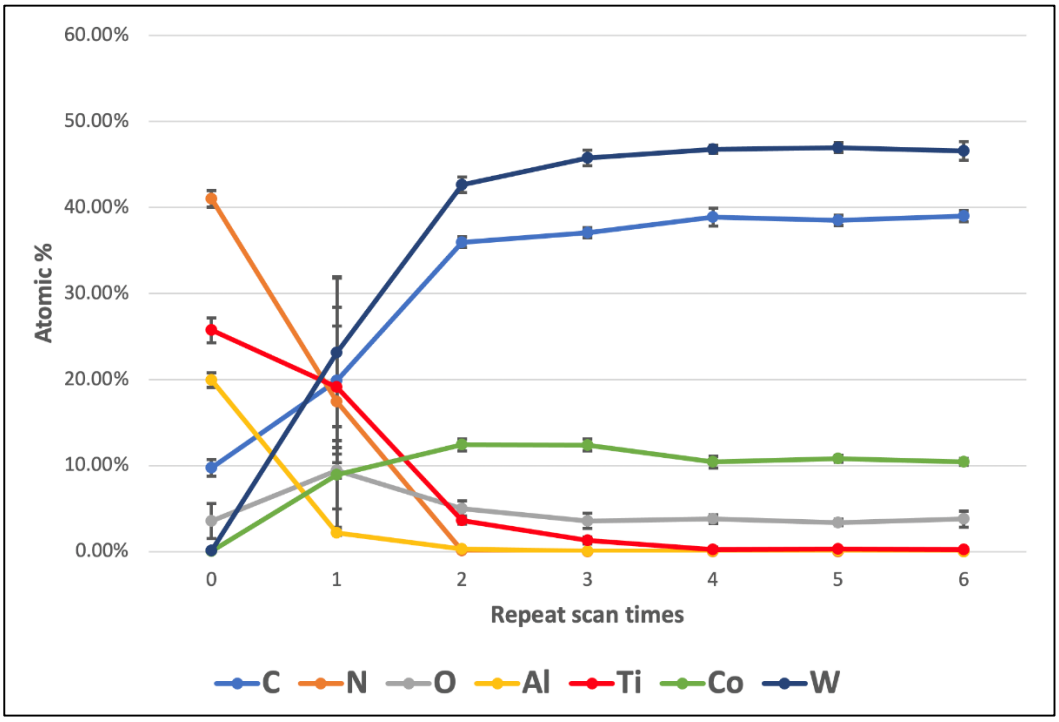

Figure 10 substrate surface chemical element composition after various laser repeat scans under optimised parameters.

From Figure 10, the element composition of TiAlN coating is shown on the zero scan point (before laser cleaning). After the first scan, the coating elements reduced dramatically and the substrate elements of W and Co started to emerge. The elements variation is quite high after the first repeat scan which indicates that the coating is partially removed and the substrate is emerging. After the second repeat scan, most of the coating materials were removed by laser ablation. The coating elements composition dropped to a very low level, the Al and N element were nearly zero, only about 3% of the Ti residual is still on the substrate. After the 4th scan, the Ti Atomic% was also dropped to nearly zero which indicates that the coating is fully removed. With further 5th and 6th repeat scan, the elements composition was maintained at a very stable level without further change. As the selected laser pulse energy is below the ablation threshold fluence of WC-Co no further ablation occurs with further laser scans.

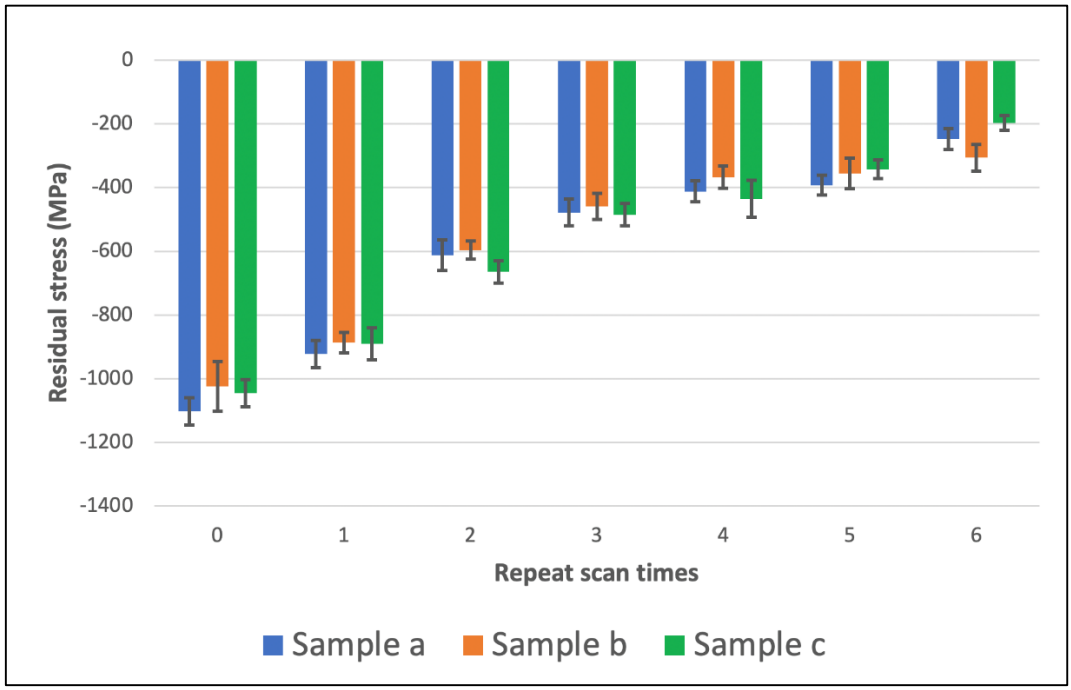

Figure 11 substrate surface residual stress after various laser repeat scans under optimised parameters.

From Figure 11, a compressive residual stress is retained on the surface with stress relief after each laser scan. The residual stress changes from about -1100 MPa to -250 MPa. As discussed earlier in section 3.5, a compressive residual stress would be beneficial for extended tool life, hence the ideal condition of de-coating is to stop laser scanning as soon as the coating is totally removed to avoid unnecessary residual stress relief. The elemental mapping showed that this happened after the fourth scan.

3.6 Modelling specific energy requirements and cleaning rate

By utilising the system specific energy consumption and processing rate data obtained in each run in Table 1, these two responses are plotted against each other and presented in Figure 12.

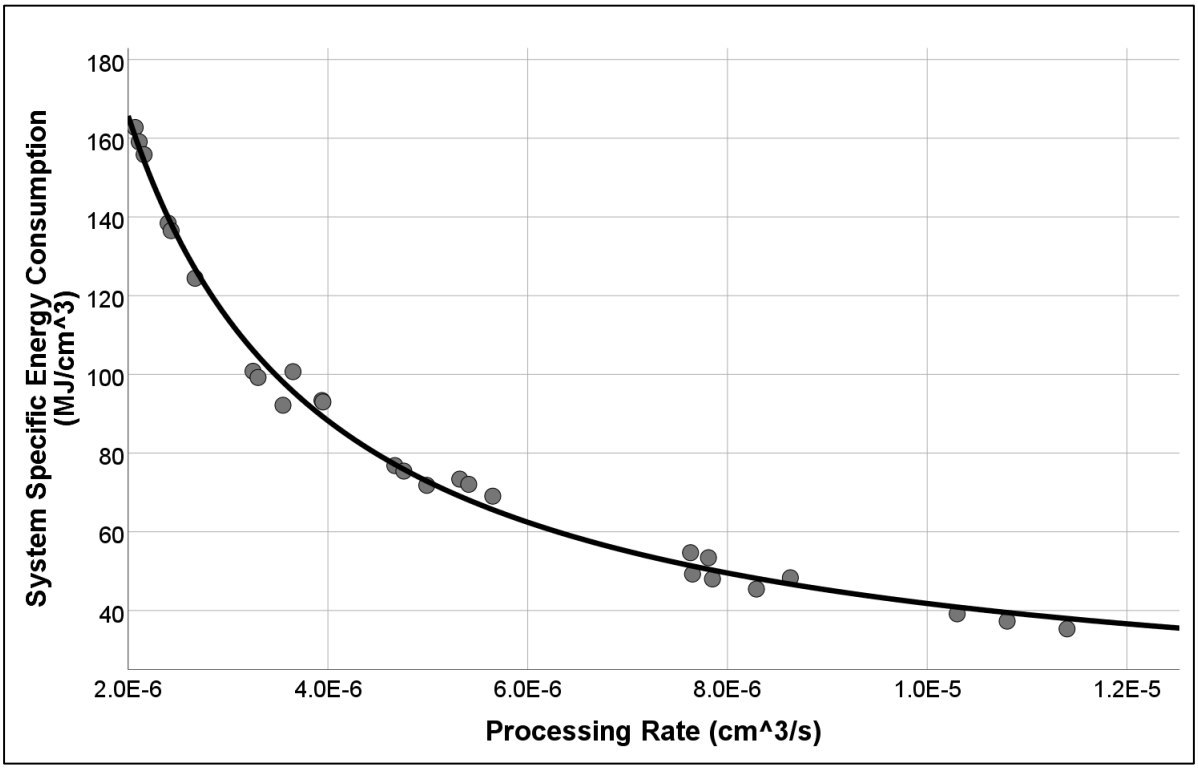

Figure 12 Laser de-coating system specific energy consumption (MJ/cm^3) vs. processing rate (cm^3/s)

A non-linear SPSS regression analysis was used to compute the trendline in Figure 12, it follows an inverse relationship in line with Equation 3.

$$\boldsymbol{E_{SEC} = C_0 + \frac{C_1}{Q}} \qquad (3)$$

Where $\boldsymbol{E_{SEC}}$ is defined as the system energy consumed to remove 1 cm^3 of material, $\boldsymbol{C_0}$ and $\boldsymbol{C_1}$ are process-specific constants, $\boldsymbol{Q}$ is the processing rate. Equation 3 also indicates two categories of the system sub-devices which consume energy. The extraction system, galvo scanner, control unit are drawing fixed active power demand during processing, which can be considered as parameter independent sub-devices, governing the magnitude of $\boldsymbol{C_0}$. The laser source is drawing different quantities of active power with relative laser beam output, which can be considered as parameter dependent sub-device, governing the magnitude of $\boldsymbol{C_1}$. The coefficients for equation 3 are summarised in Table 10. In regression analysis, the R value represents the correlation of the model fitness, this yielded R and R^2 values of 0.997 and 0.993 respectively which is quite close to a perfect correlation value of 1. Standard error was 3.29, on results ranging from 35.33 – 162.73 MJ/cm^3.

In Table 10, evaluation of the regression curve with $\boldsymbol{C_0}$ and $\boldsymbol{C_1}$ constants and their respective standard errors are both calculated and presented. The $\boldsymbol{T}$ value gives the ratio of the

Unstandardised Coefficients "***B***" (***C_0*** and ***C_1***) and their respective standard errors. This result is statistically significant, with ***Sig.***<0.001.

Table 10: Laser de-coating productivity co-efficient analysis

		Unstandardised coefficients		Standardised coefficients	***T***	***Sig.***
		B	Std. error	Beta		
1/Process rate	***C_1***	**3.10E-04**	5.00E-06	0.997	60.356	.000
Constant	***C_0***	**10.810**	1.388		7.786	.000

Then the Equation 3 can be rewritten with the value of specific constants for the investigated system as Equation 4:

$$\boldsymbol{SEC = 10.810 + \frac{0.00031}{Q}} \quad (4)$$

By using Equation 4, within known processing rate, the system specific energy consumption can be predicted.

In the research by Gutowski et al. [10,11], system specific energy consumption analysis was developed by studying the relationship between electricity requirements and processing rate in a wide choice of manufacturing processes. The specific energy consumption and processing rate for laser de-coating in Figure 12 were converted to the units of Gutowski et al. [10] used and fitted in their plot in Figure 13.

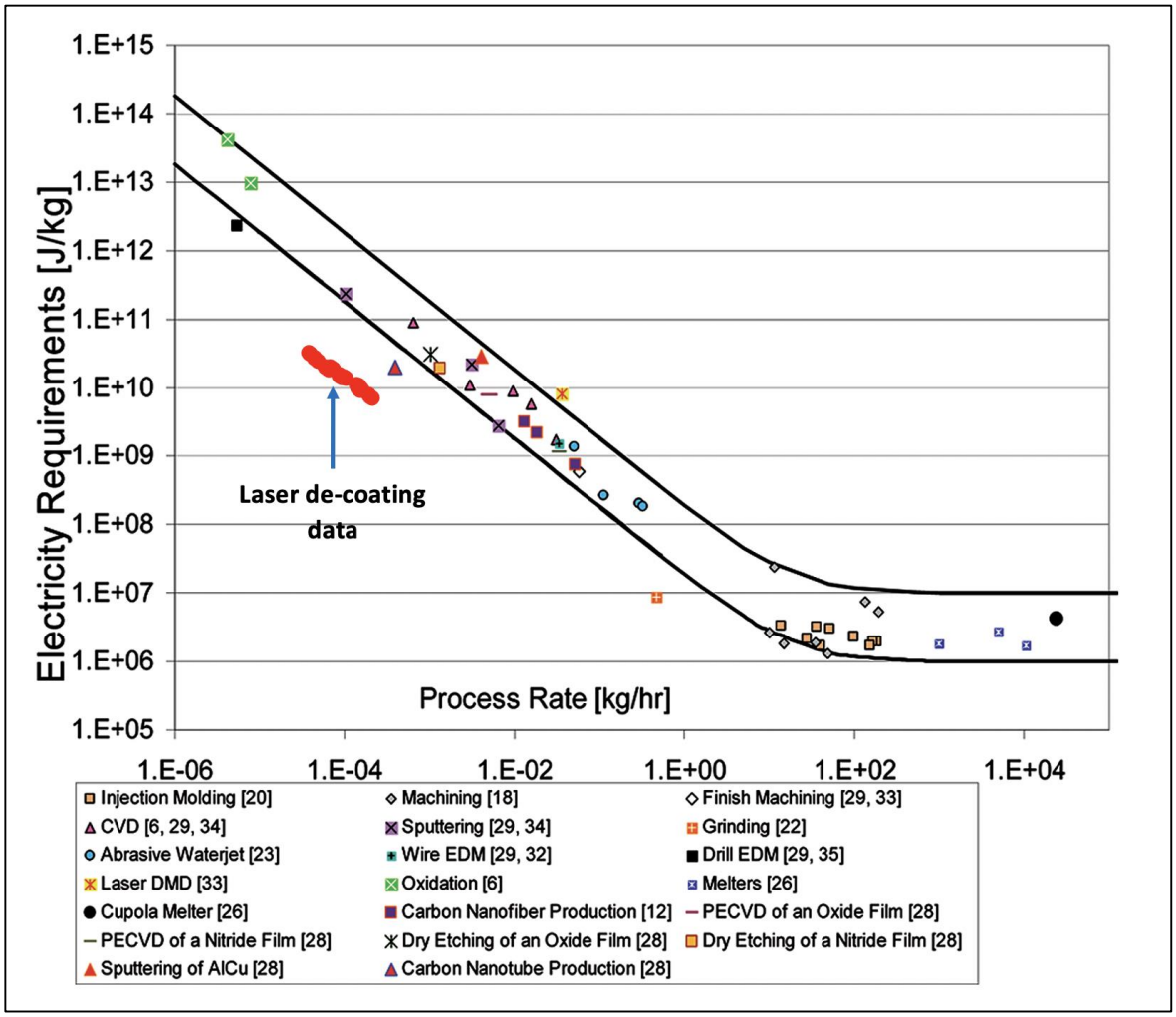

Figure 13: Specific electricity requirements for various manufacturing processes as a function of the rate of material processed [10]. (Copyright 2009 American Chemical Society)

The processes in Figure 13 are broadly classified as one class of high-precision low-volume processes (e.g. sputtering), and another of low-precision, high-volume processes (e.g. injection moulding). The laser de-coating data carried out here can be considered as high-precision, low -throughput processes. In the research by Goffin et al. [26], the specific energy consumption of laser welding system has been investigated and similar comparison applied on the Gutowski's hockey stick diagram. Since the laser welding mechanism is material melting, rather than the mainly vapourisation of laser de-coating, the specific energy consumption of laser welding is about 100 times less than laser de-coating, and processing rate is 100 times faster. It needs to be noted that, in this research the laser beam output was limited to 27 W. The processing rate can be improved by utilising parallel processing on insert batches.

4. Conclusions

In this study, the processing rate, system specific energy consumption, surface roughness, surface residual stress, chemical element composition of Ti, O, Co were studied for a range of processing parameters in laser de-coating of TiN/TiAlN coated tools. From this research, the following conclusions can be drawn:

- De-coating and re-coating of tooling is important for product life extension and hence supports a move towards a circular economy.
- The laser pulse frequency and galvo scanning speed are the two most significant parameters that can be modified in order to significantly increase the cleaning rate while simultaneously reducing the system specific energy consumption.
- The higher the pulse frequency, the more laser pulses are incident on the sample in one second, and the higher the energy input rate, which intensifies the laser-material interaction during processing, hence increasing the processing rate. A higher processing rate leads to lower cycle time and reduced energy consumption.
- This paper generated a new model and data sets for specific energy requirements for laser cleaning and this was benchmarked to other manufacturing processing. The results show that laser de-coating of hard tooling is a relatively high-precision but low-throughput process. Laser de-coating processes can be slow and energy intensive, hence more efforts needed to improve the process. For industrial applications, it is recommended to consider processing of multiple tools in one set up in order to increase the processing rate without significantly increasing the system specific energy consumption.
- By using the relative processing parameters, surface roughness ***Ra*** can be maximised or minimised for particular purposes. The analysis of the factors influencing geometric surface roughness suggests that the Gaussian laser beam influences the geometric surface profile left after cleaning.
- The signal to noise ratio in the evaluation of the surface composition changes during laser cleaning to control of the composition of Ti, O and Co suggests that the scientific interactions are more complex and are influenced by other factors beyond modelled laser input processing factors. This area requires further scientific enquiry. A theory to consider is that processing temperature and bond energies could be among key variables for the selective removal of the elements.

- A higher laser pulse energy is a significant parameter to reduce the Ti coating residue, hence promote higher surface cleanness.
- The study shows that the key elements in the carbide such as the cobalt binder is can be reduced by the cleaning process. This outcome may be beneficial for application of CVD diamond coatings, where a lower cobalt content and modified surface can help in coating adhesion and lifespan. It may be beneficial to change from TiN/TiAlN to Diamond coated tooling to improve the performance of second-generation coated tooling.
- The surface residual stress of the coated tool was compressive. Laser de-coating reduced the magnitude of the compressive residual stress but still left a compressive stress on the surface. The selection of lower pulse energy and pulse frequency can minimise the residual stress change. However, this selection is in conflict with the objective of maximising the de-coating rate and minimising the energy consumption. The assessment of the residual stress generated when maximising the cleaning rate and minimising energy consumption shows that a compressive residual stress is still retained on the surface. However the laser scanning needs to be stopped as soon as the coating is removed to limit further stress relief.
- Future research is evaluating re-coated tooling performance in cutting tests and this may through further light on the impact of reduced compressive residual stress.

Data Statement

Research data supporting this publication is reported in the Tables and Figures and supporting references.

References

[1]. Bonacchi D, Rizzi G, Bardi U, Scrivani A. Chemical stripping of ceramic films of titanium aluminum nitride from hard metal substrates. Surface and Coatings Technology. 2003;165(1):35-39.

[2]. Conde A, Cristóbal A, Fuentes G, Tate T, de Damborenea J. Surface analysis of electrochemically stripped CrN coatings. Surface and Coatings Technology. 2006;201(6):3588-3595.

[3]. Şen Y, Ürgen M, Kazmanlı K, Çakır A. Stripping of CrN from CrN-coated high-speed steels. Surface and Coatings Technology. 1999;113(1-2):31-35.

[4]. Sundar M, Whitehead D, Mativenga P, Li L, Cooke K. Excimer laser decoating of chromium titanium aluminium nitride to facilitate reuse of cutting tools. Optics & Laser Technology. 2009;41(8):938-944.

[5]. Marimuthu S, Kamara A, Whitehead D, Mativenga P, Li L. Laser removal of TiN coatings from WC micro-tools and in-process monitoring. Optics & Laser Technology. 2010;42(8):1233-1239.

[6]. Marimuthu S, Kamara A, Whitehead D, Mativenga P, Li L, Yang S et al. Laser stripping of TiAlN coating to facilitate reuse of cutting tools. Proceedings of the Institution of Mechanical Engineers, Part B: Journal of Engineering Manufacture. 2011;225(10):1851-1862.

[7]. See T, Chantzis D, Royer R, Metsios I, Antar M, Marimuthu S. Ultraviolet-Diode Pump Solid State Laser Removal of Titanium Aluminium Nitride Coating from Tungsten Carbide Substrate. Lasers in Manufacturing and Materials Processing. 2017;4(3):93-107.

[8]. Ragusich A, Taillon G, Meunier M, Martinu L, Klemberg-Sapieha J. Selective pulsed laser stripping of TiAlN erosion-resistant coatings: Effect of wavelength and pulse duration. Surface and Coatings Technology. 2013;232:758-766.

[9]. Ouyang J, Mativenga P, Liu Z, Li L. Energy consumption and process characteristics of picosecond laser de-coating of cutting tools. Journal of Cleaner Production. 2021;290:125815.

[10]. Gutowski T, Branham M, Dahmus J, Jones A, Thiriez A, Sekulic D. Thermodynamic Analysis of Resources Used in Manufacturing Processes. Environmental Science & Technology. 2009;43(5):1584-1590.

[11]. Gutowski T, Jiang S, Cooper D, Corman G, Hausmann M, Manson J et al. Note on the Rate and Energy Efficiency Limits for Additive Manufacturing. Journal of Industrial Ecology. 2017;21(S1):S69-S79.

[12]. Kara S, Li W. Unit process energy consumption models for material removal processes. CIRP Annals. 2011;60(1):37-40.

[13]. Zhou L, Li J, Li F, Meng Q, Li J, Xu X. Energy consumption model and energy efficiency of machine tools: a comprehensive literature review. Journal of Cleaner Production. 2016;112:3721-3734.

[14]. Li B, Cao H, Hon B, Liu L, Gao X. Exergy-based Energy Efficiency Evaluation Model for Machine Tools Considering Thermal Stability. International Journal of Precision Engineering and Manufacturing-Green Technology. 2020;8(2):423-434.

[15]. Roy, R.K., 2001. Design of Experiment Using the Taguchi Approach: 16 Steps to Product and Process Improvement. 1st Edn., Wiley Interscience, New York, USA., ISBN: 0471361011, pp: 560.

[16]. Peace, G.S., 1992. Taguchi Method: A Hands-on Approach. 1st Edn., Addison-Wesley Publishing, MA., USA., ISBN: 0201563118, pp: 224.

[17]. Wu B, Deng L, Liu P, Zhang F, Duan J, Zeng X. Effects of picosecond laser repetition rate on ablation of Cr12MoV cold work mold steel. Applied Surface Science. 2017;409:403-412.

[18]. Di Niso F, Gaudiuso C, Sibillano T, Mezzapesa F, Ancona A, Lugarà P. Role of heat accumulation on the incubation effect in multi-shot laser ablation of stainless steel at high repetition rates. Optics Express. 2014;22(10):12200.

[19]. Cha D, Axinte D. Transient thermal model of nanosecond pulsed laser ablation: Effect of heat accumulation during processing of semi-transparent ceramics. International Journal of Heat and Mass Transfer. 2021;173:121227.

[20]. Liu J, Lü P, Sun Y, Wang Y. Surface roughness and wettability of dentin ablated with ultrashort pulsed laser. Journal of Biomedical Optics. 2015;20(5):055006.

[21]. Barletta M, Rubino G, Gisario A. Adhesion and wear resistance of CVD diamond coatings on laser treated WC–Co substrates. Wear. 2011;271(9-10):2016-2024.

[22]. Shamsujjoha, M., Agnew, S., Brooks, J., Tyler, T. and Fitz-Gerald, J., 2015. Effects of laser ablation coating removal (LACR) on a steel substrate: Part 2: Residual stress and fatigue. Surface and Coatings Technology, 281, pp.206-214.

[23]. Harish, D., Bharatish, A., Murthy, H., Anand, B. and Subramanya, K., 2021. Investigation of thermal residual stresses during laser ablation of tantalum carbide coated graphite substrates using micro-Raman spectroscopy and COMSOL multiphysics. Ceramics International, 47(3), pp.3498-3513.

[24]. Denkena, B. and Breidenstein, B., 2008. Influence of the Residual Stress State on Cohesive Damage of PVD- Coated Carbide Cutting Tools. Advanced Engineering Materials, 10(7), pp.613-616.

[25]. Denkena, B., Breidenstein, B., Wagner, L., Wollmann, M. and Mhaede, M., 2013. Influence of shot peening and laser ablation on residual stress state and phase composition of cemented carbide cutting inserts. International Journal of Refractory Metals and Hard Materials, 36, pp.85-89.
[26]. Goffin N, Jones L, Tyrer J, Oyang J, Mativenga P, Woolley E. Mathematical Modelling for Energy Efficiency Improvement in Laser Welding. (In press) Journal of Cleaner Production.